JOC*Article*

Synthesis, Properties, and NAD$^+$-NADH-Type Redox Ability of 14-Substituted 1,3-Dimethyl-5,10-methanocycloundeca[4,5]pyrrolo-[2,3-*d*]pyrimidine-2,4(1,3*H*)-dionylium Tetrafluoroborates and Their Hydride Adducts

Kazuhiro Igarashi, Yohei Yamaguchi, Yuhki Mitsumoto, Shin-ichi Naya, and Makoto Nitta*

Department of Chemistry, Faculty of Science and Engineering, Waseda University, Shinjuku-ku, Tokyo 169-8555, Japan

nitta@waseda.jp

Received December 3, 2005

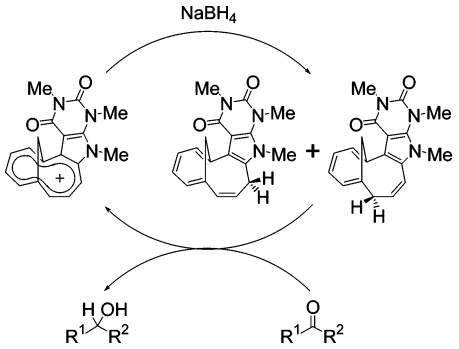

A synthesis of 14-substituted 1,3-dimethyl-5,10-methanocycloundeca[4,5]pyrrolo[2,3-*d*]pyrimidine-2,4-(1,3*H*)-dionylium tetrafluoroborates **11a,b**$^+$**·BF$_4$**$^-$ was accomplished by the methylation of 5,10-methanocycloundeca[4,5]pyrrolo[2,3-*d*]pyrimidine-2,4(1,3*H*)-dione derivatives with MeI and following anion-exchange reaction by treatment with 42% aq HBF_4. Compound **11b**$^+$**·BF$_4$**$^-$ was synthesized alternatively by the reaction of 1,6-methano[11]annulenylium tetrafluoroborate with 6-phenylamino-1,3-dimethyluracil and following oxidative cyclization reaction. Remarkable structural characteristics of **11a,b**$^+$ were clarified on inspection of the UV−vis and NMR spectral data as well as X-ray crystal analyses. The stability of cations **11a,b**$^+$ is expressed by the pK_{R+} values which were determined spectrophotometrically as 9.8 and 9.7, which are smaller by 1.4 and 1.2 pH units than those of the corresponding seven-membered ring cations, respectively; however, the values are larger by 3.6 and 3.5 pH units than that of the parent 1,6-methano[11]annulenylium ion (pK_{R+} = 6.2). The feature is rationalized on the basis of the perturbation derived from the bond fixation of the parent cation and the electron-donating ability of pyrrolopyrimidine. The electrochemical reduction of **11a**,**b**$^+$**·BF$_4$**$^-$ exhibited reduction potential at −0.58 and −0.52 (V vs Ag/$AgNO_3$) upon cyclic voltammetry (CV). Reaction of **11a**$^+$**·BF$_4$**$^-$ with hydride afforded mixures of the C13- and C11-adducts in a ratio of 81:19. Reaction of **11b**$^+$**·BF$_4$**$^-$ with hydride afforded, on the other hand, the C13-adduct as a single product. In both cations, the methano-bridge seemed to control the nucleophilic attack to the C13 favorably with exo-selectivity. The photo-induced autorecycling oxidation reactions of **11a,b**$^+$**·BF$_4$**$^-$ toward some amines under aerobic conditions were carried out to give the corresponding imines (isolated by converting to the corresponding 2,4-dinitrophenylhydrazones) with the recycling number of 1.1 to 32.2. Furthermore, as an example of the NAD$^+$-NADH models, the reduction of a pyruvate analogue and some carbonyl compounds with the hydride adducts of **11a,b**$^+$**·BF$_4$**$^-$ was accomplished for the first time to give the corresponding alcohol derivatives.

Introduction

Flavins are known to play an important role as cofactors in a wide variety of biological redox reactions.[1,2] The flavin-redox systems have been investigated extensively through synthetic model systems and theoretical calculations.[3] Among these compounds, 5-deazaflavins have been studied extensively in both enzymatic[4] and model systems,[5] in the hope of acquiring mechanistic insight into flavin-catalyzed reactions. The reactivity of 5-deazaflavins has been studied to be similar to that of

* Corresponding author. Tel: +81-(0)3-5286-3236. Fax: +81-(0)3-3208-2735.

10.1021/jo052495m CCC: $33.50
Published on Web 03/07/2006

nicotinamide.[6] Coenzyme NADH, a cofactor of L-lactate dehydrogenase, functions as an enantioselective agent that reduces pyruvate to L-lactate during anaerobic glycolysis. During the past several decades, efforts have been made to create model compounds mimicking the activity of the NAD^+-NADH redox couple.[7−17] The introduction of an optically active *N*-substituent in the amide of 1-alkylated 1,4-dihydronicotinamides, e.g., **1**, can induce modest to moderate chirality transfer toward carbonyl compounds (Figure 1).[18,19] Furthermore, Ohno and co-workers have improved considerably chirality transfer by the additional introduction of methyl groups at C2 and C4 in the NADH model, e.g., compound **2**.[20] The new chiral center at C4 controls the mode of hydride transfer. Moreover, the reduction of carbonyl compounds by using 1,5-dihydro-5-deazaflavin **3** has been reported.[21] On the basis of the above observations, we have

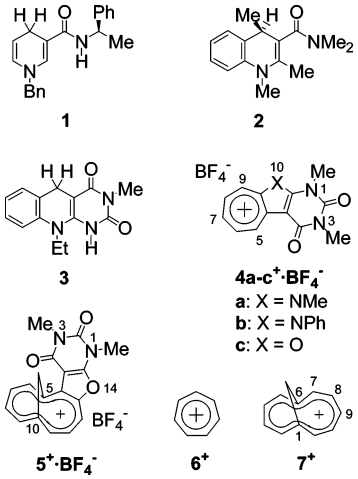

FIGURE 1. NADH model compounds and 7- and 11-membered ring cations.

previously studied the synthesis, properties, and reactivity of 10-substituted 1,3-dimethylcyclohepta[4,5]pyrrolo[2,3-*d*]pyrimidine-2,4(1,3*H*)-dionylium ions **4a,b**$^+$·BF_4^-[22] and the furan analogue **4c**$^+$·BF_4^-.[23] In these studies, it was clarified that the pyrrole analogues **4a,b** $^+$·BF_4^- have higher stability (**4a**$^+$·BF_4^-: pK_{R+} = 11.2, **4b**$^+$·BF_4^-: pK_{R+} = 10.9) as compared with **4c**$^+$·BF_4^- (pK_{R+} = ca. 6.0). In addition, novel photoinduced autorecycling oxidizing reactions of **4a**−**c**$^+$·BF_4^- toward some alcohols and amines have also been studied.[24] Thus, structural modifications of the uracil-annulated heteroazulenes such as **4a**−**c**$^+$·BF_4^- are an interesting project from the viewpoint of exploration of redox functions. Much of the motivation for studying the properties of organic molecules stems from manipulation of the primary chemical structure. One strategy for raising or lowering the HOMO and LUMO levels includes conjugation length control. Furthermore, the π-conjugation mode in polycyclic conjugated π-systems containing more than one $(4n+2)$ conjugation loop is an important subject from both theoretical and experimental viewpoints. Combination of more than one π-system can endow the original π-system with new properties. From these viewpoints, we have recently reported the synthesis, properties, and oxidizing ability of 5,10-methanocycloundeca[4,5]pyrrolo[2,3-*d*]pyrimidine-2,4(1,3*H*)-dione derivatives **10a,b**[25] (Scheme 1, vide infra) and 1,3-dimethyl-5,10-methanocycloundeca[4,5]furo[2,3-*d*]pyrimidine-2,4(1,3*H*)-dionylium tetrafluoroborate **5**$^+$·BF_4^-,[26] which is a vinylogous compound of **4c**$^+$·BF_4^-, to involve 1,6-methano[11]annulenylium ion **7**$^+$ instead of tropylium ion **6**$^+$. The cation **7**$^+$, which is an aromatic 10π-electron analogue of **6**$^+$, has higher thermodynamic stability (pK_{R+} = 6.2)[27] as compared with **6**$^+$ (pK_{R+} = 3.9).[28] Due to this property, the cation **5**$^+$·BF_4^- was expected to exhibit higher thermodynamic stability as compared with

(1) Muller, F. *Chemistry and Biochemistry of Flavoenzymes*; Muller, F., Eds.; CRC Press: Boca Raton, 1991; Vol. 1, p 1 and references therein.
(2) (a) Chiu, C. C.; Pan, K.; Jordan, F. *J. Am. Chem. Soc.* **1995**, *117*, 7027. (b) Kim, J.; Hoegy, S. E.; Mariano, P. S. *J Am. Chem. Soc*. **1995**, *117*, 100. (c) Murahashi, S.; Ono, S.; Imada, Y. *Angew. Chem., Int. Ed.* **2002**, *41*, 2366. (d) Bergstad, K.; Jonsson, S.; Bächvall, J. *J. Am. Chem. Soc*. **1999**, *121*, 10424. (e) Van Houten, K. A.; Kim, J.; Bogdan, M. A.; Ferri, D. C.; Mariano, P. S. *J. Am. Chem. Soc*. **1998**, *120*, 5864. (f) Zheng, Y.; Ornstein, R. L. *J. Am. Chem. Soc*. **1996**, *118*, 9402. (g) Breinlinger, E. C.; Keenan, C. J.; Rotello, V. M. *J. Am. Chem. Soc*. **1998**, *120*, 8606. (h) Hasford, J. J.; Rizzo, C. J. *J. Am. Chem. Soc*. **1998**, *120*, 2251. (i) Antony, J.; Medvedev, D. M.; Stuchebrukhov, A. A. *J. Am. Chem. Soc*. **2000**, *122*, 1057.
(3) Yoneda, F.; Kokel, B. In *Chemistry and Biochemistry of Flavoenzymes*; Muller, F., Ed.; CRC Press: Boca Raton, 1991; Vol. 1, p 121 and references therein.
(4) Yoneda, F.; Hirayama, R.; Yamashita, M. *Chem. Lett*. **1980**, 1157.
(5) Nitta, M.; Tajima, Y. *Synthesis* **2000**, 651.
(6) Walsh, C. *Acc. Chem. Res.* **1980**, *13*, 148.
(7) Kanomata, N.; Nakata, T. *J. Am. Chem. Soc*. **2000**, *122*, 4563.
(8) Kanomata, N. *J. Synth. Org. Chem. Jpn*. **1999**, *57*, 512.
(9) Murakami, Y.; Kikuchi, J.; Hisaeda, Y.; Hayashida, O. *Chem. Rev.* **1996**, *96*, 721.
(10) Dupas, G.; Levacher, V.; Bourguignon, J.; Quéguiner, G. *Heterocyles* **1994**, *39*, 405.
(11) Burgess, V. A.; Davies, S. G.; Skerlj, R. T. *Tetrahedron*: *Asynmmetry* **1991**, *2*, 299.
(12) (a) Ohno, A.; Ikeuchi, M.; Kimura, T.; Oka, S. *J. Am. Chem. Soc*. **1979**, *101*, 7036. (b) Mikata, Y.; Hayashi, K.; Mizukami, K.; Matsumoto, S.; Yano, S.; Yamazaki, N.; Ohno, A. *Tetrahedron Lett.* **2000**, *41*, 1035. (c) de Kok, P. M. T.; Bastiaansen, L. A. M.; van Lier, P. M.; Vekemans, J. A. J. M.; Buck, H. M. *J. Org. Chem*. **1989**, *54*, 1313. (d) Meyers, A. I.; Oppenlaender, T. *J. Am. Chem. Soc*. **1986**, *108*, 1989. (e) Meyers, A. I.; Brown, J. D. *J. Am. Chem. Soc*. **1987**, *109*, 3155.
(13) (a) Combret, Y.; Torché, J. J.; Pié, N.; Duflos, J.; Dupas, G.; Bourguignon, J.; Quéguiner, G. *Tetrahedron* **1991**, *47*, 9369. (b) Combret, Y.; Torché, J. J.; Binay, P.; Dumpas, G.; Bourguignon, J.; Quéguiner, G. *Chem. Lett.* **1991**, 125. (c) Combret, Y.; Duflos, J.; Dupas, G.; Bourguignon, J.; Quéguiner, G. *Tetrahedron* **1993**, *49*, 5237.
(14) (a) Burgess, V. A.; Davies, S. G.; Skerlj, R. T.; Whittaker, M. *Tetrahedron: Asymmetry* **1992**, *3*, 871. (b) Burgess, V. A.; Davies, S. G.; Skerlj, R. T. *J. Chem. Soc., Chem. Commun*. **1990**, 1759.
(15) (a) Seki, M.; Baba, N.; Oda, J.; Inouye, Y. *J. Am. Chem. Soc*. **1981**, *103*, 4613. (b) Hoshide, F.; Ohi, S.; Baba, N.; Oda, J.; Inouye, Y. *Agric. Biol. Chem.* **1982**, *46*, 2173. (c) Seki, M.; Baba, N.; Oda, J.; Inouye, Y. *J. Org. Chem.* **1983**, *48*, 1370.
(16) (a) de Vries, J. G.; Kellogg, R. M. *J. Am. Chem. Soc*. **1979**, *101*, 2759. (b) Jouin, P.; Troostwijk, C. B.; Kellogg, R. M. *J. Am. Chem. Soc.* **1981**, *103*, 2091.
(17) (a) Imanishi, T.; Hamano, Y.; Yoshikawa, H.; Iwata, C. *J. Chem. Soc., Chem. Commun*. **1988**, 473. (b) Obika, S.; Nishiyama, T.; Tatematsu, S.; Miyashita, K.; Iwata, C.; Imanishi, T. *Tetrahedron* **1997**, *53*, 593. (c) Obika, S.; Nishiyama, T.; Tatematsu, S.; Miyashita, K.; Imanishi, T. *Chem. Lett*. **1996**, 853.
(18) Ohnishi, Y.; Kagami, M.; Ohno, A. *J. Am. Chem. Soc*. **1975**, *97*, 4766.
(19) Endo, T.; Hayashi, Y. Okawara, M. *Chem. Lett*. **1977**, 391.
(20) Ohno, A.; Kashiwagi, M.; Ishihara, Y.; Ushida, S.; Oka, S. *Tetrahedron* **1986**, *42*, 961. Mikata, Y.; Mizukami, K.; Hayashi, K.; Matsumoto, S.; Yano, S.; Yamazaki, N.; Ohno, A. *J. Org. Chem*. **2001**, *66*, 1590.
(21) (a) Yoneda, F.; Sakuma, Y.; Nitta, Y. *Chem. Lett*. **1978**, 1177. (b) Yoneda, F.; Kuroda, K.; Tanaka, K. *Chem. Commun*. **1984**, 1194.
(22) Naya, S.; Nitta, M. *Tetrahedron* **2003**, *59*, 7291.
(23) (a) Naya, S.; Miyama, H.; Yasu, K.; Takayasu, T.; Nitta, M. *Tetrahedron* **2003**, *59*, 1811−1821. (b) Naya, S.; Nitta, M. *Tetrahedron* **2003**, *59*, 3709.
(24) Naya, S.; Nitta, M. *Tetrahedron* **2004**, *60*, 9139.
(25) Mitsumoto, Y.; Nitta, M. *J. Org. Chem.* **2004**, *69*, 1256.
(26) Naya, S.; Warita, M.; Mitsumoto, Y.; Nitta, M. *J. Org. Chem.* **2004**, *69*, 9184.
(27) (a) Grimme, W.; Hoffmann, H.; Vogel, E. *Angew. Chem., Int. Ed. Engl*. **1965**, *4*, 354. (b) Vogel, E.; Feldmann, R.; Düwel, H. *Tetrahedron Lett.* **1970**, *1*, 1941.

SCHEME 1[a]

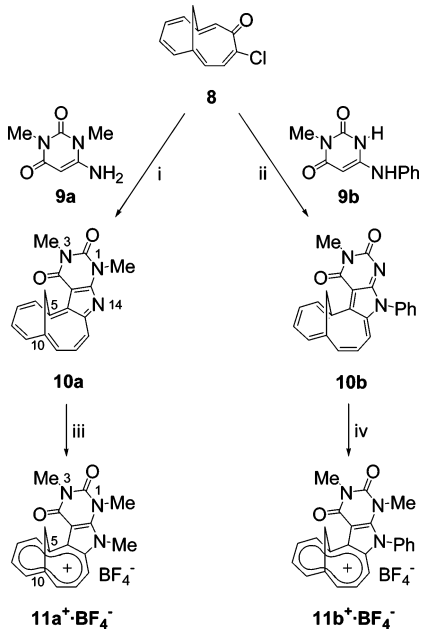

[a] Reagents and conditions: (i) AcOH, 60 °C, 25 h; (ii) AcOH, 80 °C, 54 h; (iii) (a) MeI, $(CH_2Cl)_2$, 100 °C, 5 days, (b) 42% aq HBF_4, Ac_2O, 0 °C, 30 min; (iv) (a) MeI, $(CH_2Cl)_2$, 100 °C, 2 days, (b) 42% aq HBF_4, Ac_2O, 0 °C, 30 min.

SCHEME 2[a]

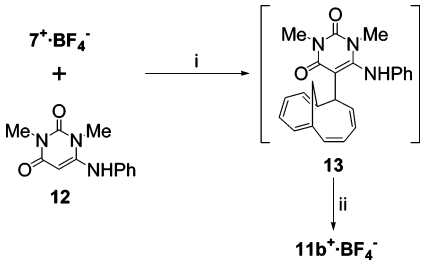

[a] Reagents and conditions: (i) K_2CO_3, CH_3CN, rt, 2 days; (ii) (a) DDQ, CH_3CN, rt, 1 h, (b) 42% aq HBF_4, Ac_2O, 0 °C, 30 min.

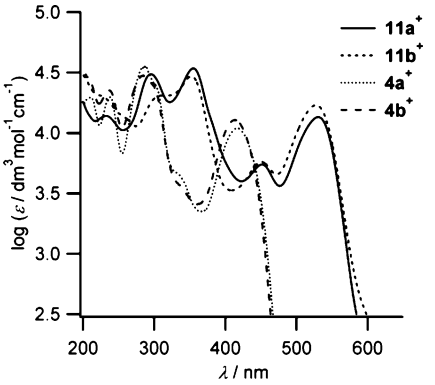

FIGURE 2. UV−vis spectra of **11a,b**$^+$**·BF**$_4^-$ and **4a,b**$^+$**·BF**$_4^-$.

4c$^+$**·BF**$_4^-$; however, it exhibited lower thermodynamic stability ($pK_{R+} = 4.6$). Furthermore, the reaction of **5**$^+$**·BF**$_4^-$ with $NaBD_4$ shows that the methano-bridge controls the nucleophilic attacks to occur with exo-selectivity at the C11 and C13 positions. Thus, study of the methano-bridged compounds is an interesting project from the viewpoint of exploration of novel chiral auxiliaries. In this study, we report the synthesis, properties, and structural details of 14-substituted 1,3-dimethyl-5,10-methanocycloundeca[4,5]pyrrolo[2,3-*d*]pyrimidine-2,4(1,3*H*)-dionylium tetrafluoroborates **11a,b**$^+$**·BF**$_4^-$, which are derived from annulation of **7**$^+$ with pyrrolo[2,3-*d*]pyrimidine-1,3(2,4*H*)-dione. The photoinduced oxidizing reaction of **11a,b**$^+$**·BF**$_4^-$ toward some amines was studied as well. Furthermore, as an exploration of NAD$^+$−NADH type redox functions, the reduction of a pyruvate analogue and some carbonyl compounds with the hydride-adducts of **11a,b**$^+$**·BF**$_4^-$ was studied for the first time to give the corresponding alcohol derivatives.

Results and Discussion

Synthesis. We have previously reported a convenient preparation of 5,10-methanocycloundeca[4,5]pyrrolo[2,3-*d*]pyrimidine-2,4(1,3*H*)-dione derivatives **10a**,**b**[25] by the thermal reaction of 11-chloro-3,8-methano[11]annulenone **8** with 6-aminouracil derivatives **9a**,**b**. In this work, 14-substituted 1,3-dimethyl-5,10-methanocycloundeca[4,5]pyrrolo[2,3-*d*]pyrimidine-2,4-(1,3*H*)-dionylium tetrafluoroborates **11a,b**$^+$**·BF**$_4^-$ were prepared from **10a**,**b**. Methylation of **10a**,**b** with MeI in $(CH_2Cl)_2$ under reflux, and subsequent anion-exchange reaction consisting of treatment with 42% aq HBF_4 in Ac_2O at 0 °C afforded desired compounds **11a,b**$^+$**·BF**$_4^-$ in 98% and 100% yields, respectively (Scheme 1). On the other hand, **11b**$^+$**·BF**$_4^-$ was alternatively synthesized starting from 1,6-methano[11]annulenylium tetrafluoroborate **7**$^+$**·BF**$_4^-$ [27] (Scheme 2). The reaction of **7**$^+$**·BF**$_4^-$ with 6-phenylamino-1,3-dimethyluracil **12** in the presence of K_2CO_3 furnished compound **13**, which is unstable on TLC (SiO_2 and Al_2O_3). Thus, without further purification, oxidative cyclization reaction of **13** with DDQ and following anion-exchange reaction using 42% aq HBF_4 in Ac_2O at 0 °C was carried out to give **11b**$^+$**·BF**$_4^-$ (81% yield based on **7**$^+$**·BF**$_4^-$).

Properties of 11a,b$^+$**·BF**$_4^-$**.** Compounds **11a,b**$^+$**·BF**$_4^-$ were fully characterized on the basis of the ^{1}H NMR, ^{13}C NMR, IR, UV−vis, and mass spectral data as well as elemental analyses and X-ray crystal analysis. The mass spectra of **11a,b**$^+$**·BF**$_4^-$ exhibited the correct $M^+ - BF_4^-$ ion peaks, which were indicative of the cationic structures of these compounds. The characteristic absorption bands for the counterion of BF_4^- were observed at 1084 cm^{-1} in their IR spectra. The UV−vis spectra of **11a,b**$^+$**·BF**$_4^-$ in CH_3CN are similar, and they are shown in Figure 2, together with those of **4a,b**$^+$**·BF**$_4^-$.[22] The longest wavelength absorption maxima (λ_{max}) of **11a,b**$^+$**·BF**$_4^-$ exhibited a red-shift by 114 nm as compared with those of **4a,b**$^+$**·BF**$_4^-$, respectively, due to the elongated π-conjugation.

The ^{1}H NMR spectra of **11a,b**$^+$**·BF**$_4^-$ are noteworthy since the chemical shifts of bridged-annulene systems are quite useful in determining such structural properties as diatropicity and bond alternation. Unambiguous proton assignment was made by analyzing ^{1}H NMR and H−H COSY spectra. The chemical shifts of bridge protons and selected coupling constants of **11a,b**$^+$**·BF**$_4^-$ are shown in Figure 3, together with those of the reference compounds **10a,b**.[25] The large geminal coupling constant of the methylene protons ($J_{E,Z} = 12.2$ Hz) supports the absence of a norcaradiene structure for **11a,b**$^+$**·BF**$_4^-$. Furthermore, the bridge protons of **11a,b**$^+$**·BF**$_4^-$ appear at very higher field (δ −0.54 to −1.44), and the peripheral protons appear in lower field of the aromatic region (δ 8.06 to 10.29). These features indicate that **11a,b**$^+$**·BF**$_4^-$ have a large diatropic

(28) Okamoto, K.; Takeuchi, K.; Komatsu, K.; Kubota, Y.; Ohara, R.; Arima, M.; Takahashi, K.; Waki Y.; Shirai, S. *Tetrahedron* **1983**, *39*, 4011 and references therein.

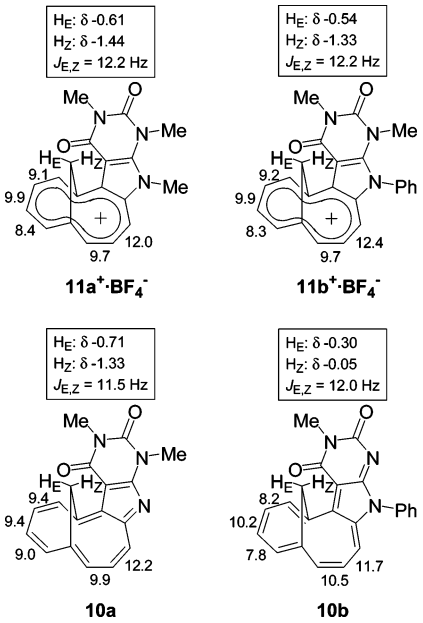

FIGURE 3. Chemical shifts of bridge protons and selected coupling constants of **11a,b**$^+$**·BF$_4^-$** and reference compounds **10a,b**.

ring current.[29] It is interesting that the signals of H_Z of **11a,b**$^+$**·BF$_4^-$** appear at higher field (δ −1.44 and −1.33, respectively) as compared with those of H_E (δ −0.61 and −0.54, respectively). This tendency is similar to that of **10a**. In addition, the signals of the N1Me and the H13 of **11b**$^+$**·BF$_4^-$** appeared at higher field (δ 3.14 and 8.41, respectively) as compared with those of **11a**$^+$**·BF$_4^-$** (δ 3.96 and 8.99, respectively). This tendency suggests that the N1Me and the H13 of **11b**$^+$**·BF$_4^-$** are located at the shielding region of the phenyl group in the pyrrole ring, and thus, the phenyl group would twist against the plane of the π-system. The vicinal coupling constants of the aromatic perimeter protons suggest that the C6−C7−C8−C9 moiety exhibits small bond alternation in **11a**$^+$**·BF$_4^-$** [$J_{6,7}$ (9.1 Hz), $J_{7,8}$ (9.9 Hz), $J_{8,9}$ (8.4 Hz)] and **11b**$^+$**·BF$_4^-$** [$J_{6,7}$ (9.2 Hz), $J_{7,8}$ (9.9 Hz), $J_{8,9}$ (8.3 Hz)]. This feature is similar to that of compound **10a**. In contrast, it is noteworthy that the vicinal coupling constants of the C11−C12−C13 moiety exhibits large bond alternation in **11a**$^+$**·BF$_4^-$** [$J_{11,12}$ (9.7 Hz) < $J_{12,13}$ (12.0 Hz)] and **11b**$^+$**·BF$_4^-$** [$J_{11,12}$ (9.7 Hz) < $J_{12,13}$ (12.4 Hz)]. While the C11−C12−C13 moiety in **10b** shows a small bond alternation, there is a large bond alternation at that of **10a**. The ^{13}C NMR spectral data for **11a**$^+$**·BF$_4^-$** were fully assigned by using the H−C COSY spectra (HMQC and HMBC). Concerning the 11-membered ring, the signals of the C13 appeared at much higher field (δ_c 128.6) as compared with those of the other carbons. Moreover, the signals of the C11 appeared at much lower field (δ_c 152.6) as compared with those of the other carbons, suggesting that the positive charge may be localized at this position. This tendency is observed similarly for **11b**$^+$**·BF$_4^-$**.

A single crystal of **11a**$^+$**·BF$_4^-$** was obtained by recrystallization from CH_3CN/Et_2O, and thus, X-ray crystal analysis was carried out to clarify the structural details of **11a**$^+$**·BF$_4^-$**. X-ray crystal analysis of reference compound **10a** was also carried out. The ORTEP drawing of **11a**$^+$**·BF$_4^-$** is shown in Figure 4, together with that of **10a**. The counteranion is omitted for clarity in the ORTEP drawing, and selected bond lengths of **11a**$^+$ and **10a** are also summarized in Figure 4. The single crystals of **11a**$^+$**·BF$_4^-$** and **10a** are a racemic mixture, respectively, and not a conglomerate, and thus, optical resolution through recrystallization seems to be difficult. While the pyrrolopyrimidine ring moiety of **10a** has a nearly planar structure, small deformation of the 11-membered ring from planarity is observed (Figure 4, side view). On the contrary, owing to the steric hindrance between two methyl groups, small deformation of the pyrimidinedione ring moiety of **11a**$^+$ from planarity is observed (Figure 4, side view), while 11-membered ring of **11a**$^+$ has a nearly planar structure. Moreover, the bond lengths of the 11-membered ring of **11a**$^+$ are almost equal, exhibiting no bond length alternation. In consideration of the results of X-ray crystal analysis and NMR spectra, the canonical structures **11a**$^+$**-A**, **11a**$^+$**-B**, and **11a**$^+$**-C** are important for **11a**$^+$ (Figure 5). Furthermore, the bond length of the N1−C18 is shorter than that of the N1−C10, suggesting that the contribution of **11a**$^+$**-D** is less important.

The affinity of the carbocation toward hydroxide ions expressed by the pK_{R+} value is a common criterion of carbocation stability.[30] The pK_{R+} values of cations **11a,b**$^+$ were determined spectrophotometrically in buffer solutions prepared in 50% aqueous CH_3CN and are summarized in Table 1, along with those of the reference compounds **4a**−**c**$^+$,[22,23] **5**$^+$,[26] **6**$^+$,[28] and **7**$^+$.[27] The pK_{R+} values of **4a**−**c**$^+$are much larger than that of **6**$^+$, and they are in the order **4a**$^+$ > **4b**$^+$ > **4c**$^+$, indicating that the electron-donating ability of pyrrolopyrimidine is larger than that of furopyrimidine and destabilizing effect by double bond fixation by annulation is not observed. On the other hand, the pK_{R+} values of **11a,b**$^+$ were determined to be 9.8 and 9.7, which are larger by 5.2 and 5.1 pH unit than that of **5**$^+$ (pK_{R+} = 4.6), respectively, reflecting large electron-donating ability of pyrrolopyrimidine as compared with that of furopyrimidine. The cation **7**$^+$, which is an aromatic 10π-electron analogue of **6**$^+$, has higher thermodynamic stability (pK_{R+} = 6.2)[27] than that of **6**$^+$ (pK_{R+} = 3.9);[28] however, the pK_{R+} values of **11a,b**$^+$ and **5**$^+$ are smaller by 1.4, 1.2, and 1.4 pH unit than those of **4a**−**c**$^+$, respectively. Thus, the feature is rationalized on the basis of large perturbation derived from the double bond fixation of the parent cation **7**$^+$. Since the C7−C8 bond of **7**$^+$ has a small bond order (small double bond character),[31] the pyrrolopyrimidine and furopyrimidine-annulation onto **7**$^+$ at this position (introduction of a double bond) seems to cause larger perturbation[32] than the introduction of a double bond onto a fully delocalized double bond of **6**$^+$. This electronic effect would act as a considereble destabilizing effect of parent cation **7**$^+$ as compared with that of **6**$^+$.

The reduction potentials of **11a,b**$^+$ were determined by cyclic voltammentry (CV) in CH_3CN. The reduction waves were irreversible under the conditions of the CV measurements; the peak potentials are summarized in Table 1, together with those of the reference compounds **4a**−**c**$^+$,[22,23] **5**$^+$,[26] **6**$^+$,[28] and **7**$^+$.[27] The $E1_{red}$ of **11a,b**$^+$ are more positive by 0.29 and 0.32 V than those of **4a,b**$^+$, respectively, suggesting the elongated π-conjugation of **11a,b**$^+$. Furthermore, the more negative $E1_{red}$ of **11a,b**$^+$ as compared with those of **5**$^+$, **6**$^+$, and **7**$^+$ would be comparable with the higher pK_{R+} values of **11a,b**$^+$.[22] The irreversible nature is probably due to the formation of a radical

(29) Vogel, E. *Chem. Soc. Spec. Publ*. **1967**, *21*, 113.

(30) Freedman, H. H. In *Carbonium Ions;* Olah, G. A., Schleyer, P., Eds.; Wiley-Insterscience: New York, 1973.

(31) Destro, R.; Simonetta, M. *Acta Crystallogr*. **1979**, *B35*, 1846.

(32) Yamane, K.; Yamamoto, H.; Nitta, M. *J. Org. Chem.* **2002**, *67*, 8114.

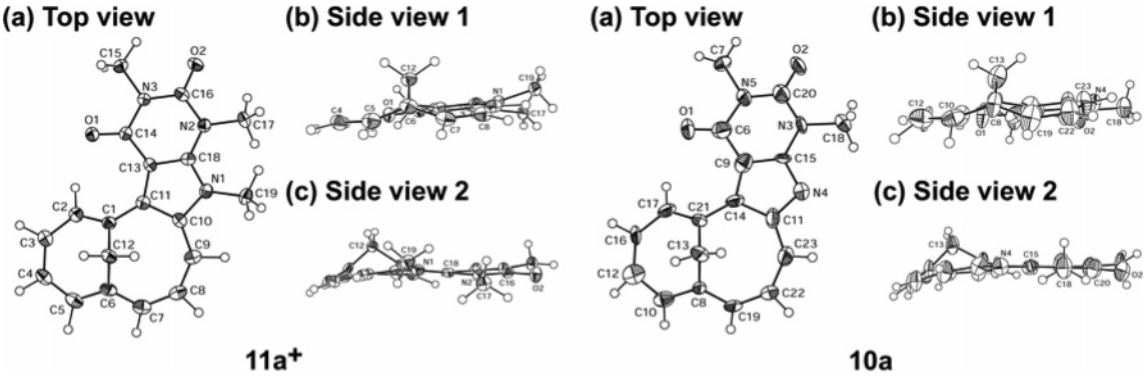

FIGURE 4. ORTEP drawings of **11a**$^+$**·BF**$_4^-$ and **10a** with thermal ellipsoid plot (50% probability). Selected bond lengths (Å) of **11a**$^+$**·BF**$_4^-$: N1−C10 1.408(4), N1−C18 1.355(4), N2−C18 1.363(4), C1−C2 1.392(4), C2−C3 1.408(5), C3−C4 1.395(5), C4−C5 1.392(5), C5−C6 1.387-(5), C6−C7 1.398(5), C7−C8 1.394(5), C8−C9 1.402(5), C9−C10 1.398(4), C10−C11 1.457(4), C11−C13 1.408(4), C13−C18 1.393(4). Selected bond lengths (Å) of **10a**: N3−C15 1.37(3), N4−C15 1.36(2), N4−C11 1.37(3), C9−C14 1.40(3), C9−C15 1.40(2), C11−C14 1.47(2), C14−C21 1.42(3), C21−C17 1.37(2), C17−C16 1.42(3), C16−C12 1.39(3), C12−C10 1.39(2), C10−C8 1.42(3), C8−C19 1.38(2), C19−C22 1.38(3), C22−C23 1.42(3), C23−C11 1.39(2).

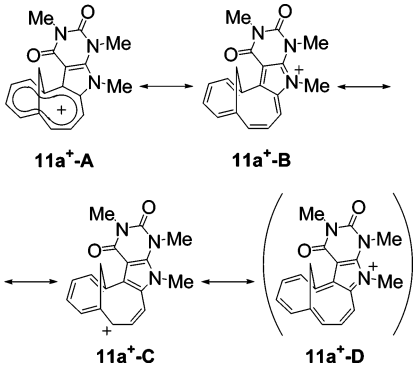

FIGURE 5. Resonance structure of **11a**$^+$.

TABLE 1. pK_{R+} Values and Reduction Potentials[a] of Cations 11a,b$^+$ [b] and Reference Compounds 4a−c$^+$, 5$^+$, 6$^+$, and 7$^+$

compd	pK_{R+}	reduction potential ($E1_{red}$)
11a$^+$	9.8	−0.58
11b$^+$	9.7	−0.52
4a$^+$ [c]	11.2	−0.87
4b$^+$ [c]	10.9	−0.84
4c$^+$ [d]	ca. 6.0	−0.58
5$^+$ [e]	4.6	−0.39
6$^+$ [f]	3.9	−0.51
7$^+$ [g]	6.2	−0.42[e]

[a] V vs Ag/AgNO$_3$; cathodic peak potential. [b] Salts **11a,b**$^+$**·BF**$_4^-$ were used for the measurement. [c] Reference 22. [d] Reference 23. [e] Reference 26. [f] Reference 28. [g] Reference 27.

species and its dimerization, as reported to be a typical property of uracil-annulated heteroazulenylium ions **4a−c**$^+$ [22,23] and **5**$^+$.[26]

Autorecycling Oxidation of Some Amines. Compounds **4a−c**$^+$**·BF**$_4^-$ act as a catalyst for oxidation of some alcohols under photoirradiation.[22,23] Moreover, compounds **10a,b** and **5**$^+$**·BF**$_4^-$ have been reported to undergo autorecycling oxidation toward some amines under photoirradiation.[25,26] In this context, we studied the oxidizing ability of **11a,b**$^+$**·BF**$_4^-$ under similar conditions. Although **11a,b**$^+$**·BF**$_4^-$ did not show oxidizing ability toward alcohols, they have oxidizing ability toward benzylamine, 1-phenylethylamine, hexylamine, and cyclohexylamine to give the corresponding imines under aerobic and photoirradiation conditions. In the amine oxidation, imine is produced at first; however, it reacts with another amine to result in the formation of another imine and NH$_3$ (Scheme 3). Then the reaction mixture was diluted with ether and filtered and the

SCHEME 3[a]

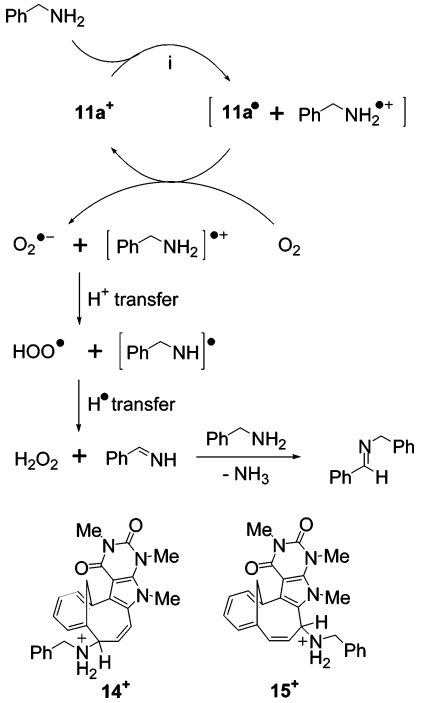

[a] Reagents and conditions: (i) *hν*, aerobic, CH$_3$CN, rt, 16 h.

filtrate was treated with 2,4-dinitrophenylhydrazine in 6% HCl to give 2,4-dinitrophenylhydrazone of the corresponding carbonyl compound. Direct irradiation of the amines in the absence of **11a,b**$^+$**·BF**$_4^-$ (named "blank") gives the corresponding imines in small amounts. Thus, the recycling number is calculated by subtraction of the "blank" yield from the yield of the imine in the presence of **11a,b**$^+$**·BF**$_4^-$, and the results are summarized in Table 2, together with those of **4a,b**$^+$**·BF**$_4^-$.[22] The recycling numbers of **11a,b**$^+$**·BF**$_4^-$ support the proceeding of autorecycling oxidation. The reactions with **11a,b**$^+$**·BF**$_4^-$ gave lower recycling numbers as compared with those of **4a,b**$^+$**·BF**$_4^-$, respectively. As a representative, the postulated reaction pathways for the oxidation of benzylamine by **11a**$^+$**·BF**$_4^-$ are depicted in Scheme 3. We propose that photoinduced homolytic cleavage of the initially formed amine-adducts **14**$^+$ and/or **15**$^+$, which is detected by UV−vis spectra as shown in Figure 6, probably occurs to generate a radical **11a**$^•$ and a radical cation

TABLE 2. Autorecycling Oxidation of Some Amines by 11a,b$^+$·BF$_4^-$ under Aerobic and Photoirradiation Conditions[a]

entry	compd	amine	yield/μmol[b,c]	recycling no.[d]
1	**11a**$^+$·BF$_4^-$	$PhCH_2NH_2$	139.9	28.0
2	**11a**$^+$·BF$_4^-$	$PhCH(Me)NH_2$	96.7	19.3
3	**11a**$^+$·BF$_4^-$	hexylamine	25.0	5.0
4	**11a**$^+$·BF$_4^-$	cyclohexylamine	43.2	8.6
5	**11b**$^+$·BF$_4^-$	$PhCH_2NH_2$	61.2	12.2
6	**11b**$^+$·BF$_4^-$	$PhCH(Me)NH_2$	74.7	14.9
7	**11b**$^+$·BF$_4^-$	hexylamine	5.7	1.1
8	**11b**$^+$·BF$_4^-$	cyclohexylamine	28.8	5.8
9	**4a**$^+$·BF$_4^-$	$PhCH_2NH_2$	150.0	30.0
10	**4a**$^+$·BF$_4^-$	$PhCH(Me)NH_2$	118.4	23.7
11	**4b**$^+$·BF$_4^-$	$PhCH_2NH_2$	208.8	41.8
12	**4b**$^+$·BF$_4^-$	$PhCH(Me)NH_2$	178.8	35.7

[a] A CH_3CN (16 mL) solution of compounds **11a,b**$^+$·BF$_4^-$ (5 μmol) and amine (2.5 mmol, 500 equiv) was irradiated by RPR-100, 350 nm lamps under aerobic conditions for 16 h. [b] Isolated by converting to the corresponding 2,4-dinitrophenylhydrazone. [c] The yield is calculated by subtraction of the "blank" yield from the total yield. [d] Recycling number of **11a,b**$^+$·BF$_4^-$ and **4a,b**$^+$·BF$_4^-$.

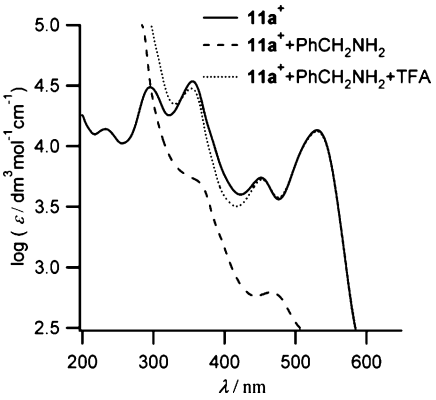

FIGURE 6. UV−vis spectra of **11a**$^+$·BF$_4^-$ with $PhCH_2NH_2$.

$PhCH_2NH_2^{\bullet+}$. In the presence of oxygen, an electron transfer from **11a**$^\bullet$ to O_2 may occur to give the radical ion pair [$PhCH_2NH_2^{\bullet+}O_2^{\bullet-}$] and **11a**$^+$. Then proton transfer from $PhCH_2NH_2^{\bullet+}$ to $O_2^{\bullet-}$ may occur, followed by formation of products H_2O_2 and PhCH=NH, which reacts with another amine to result in the formation of $PhCH{=}NCH_2Ph$ and NH_3.[25,33] Alternatively, the present autorecycling oxidation may proceed via an electron transfer from benzylamine to excited cation **11a**$^+$ which would occur to produce a radical **11a**$^\bullet$ and $PhCH_2NH_2^{\bullet+}$.[25] Then, they would follow the proposed reaction pathways shown above.

Reaction of 11a,b$^+$·BF$_4^-$ with NaBH$_4$. While the reaction of **4a,b**$^+$·BF$_4^-$ with $NaBH_4$ proceeded at the C5, C7, and C9 positions to give mixtures of three regioisomers **16a**−**18a** and **16b**−**18b** in a ratio of 15:4:81 and 25:7:68, respectively (Scheme 4),[22] the reaction of **5**$^+$·BF$_4^-$ proceeded at the C13 and C11 positions to give a mixture of **19** and **20** in a ratio of 89:11.[26] In contrast, a reaction of **11a**$^+$·BF$_4^-$ with $NaBH_4$ in CH_3CN was carried out to afford hydride adducts **21a** and **22a** in a ratio of 81:19, quantitative yield (Scheme 4). The ratio was determined by the ^{1}H NMR spectrum of the mixture. The reaction of **11b**$^+$·BF$_4^-$ with $NaBH_4$ in CH_3CN was also carried out to give only the C13-adduct **21b**, and the C11-adduct **22b** was not obtained. There is well-known tendency for double bond fixation in the methano[11]annulene system to favor a cycloheptatriene moiety predominantly over a 1,6-dimethylenecyclohepta-2,4-diene moiety.[34] Thus, the formation of **21a**, **22a**,

(33) Fukuzumi, S.; Kuroda, S. *Res. Chem. Intermed.* **1999**, 25, 789.

SCHEME 4[a]

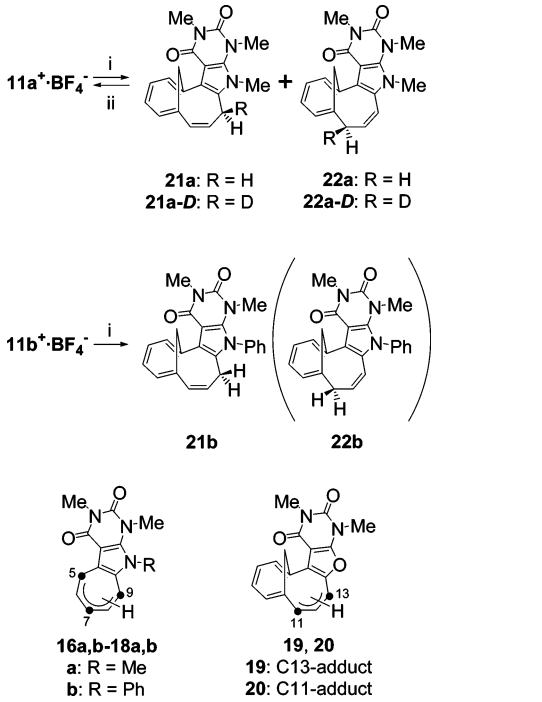

[a] Reagents and conditions: (i) $NaBH_4$, CH_3CN, rt, 30 min; (ii) (a) DDQ, CH_2Cl_2, rt, 30 min, (b) 42% aq HBF_4, Ac_2O, 0 °C, 30 min.

and **21b** would be ascribed to the stability of both the cycloheptatriene moiety and the closed pyrrole ring. The feature is similar to the reaction of **5**$^+$·BF$_4^-$ with $NaBH_4$, in which the ratio of the C13-adduct **19** was larger than that of the C11-adduct **20**.[26] To clarify endo-exo selectivity, a reaction of **11a**$^+$·BF$_4^-$ with $NaBD_4$ in CH_3CN was carried out to give a mixture of C13-adduct **21a-*D***, C11-adduct **22a-*D***, and **21a** in a ratio of 83:2:15 in quantitative yield. The ratio was determined by the ^{1}H NMR spectrum of the mixture. Since $NaBD_4$ used for the reaction is of 96% deuterium content, the reaction of **11a**$^+$·BF$_4^-$ with the remaining hydride would give compound **21a**. The structural assignments of **21a**, **22a**, **21a-*D***, and **22a-*D*** were based on the NMR and HRMS spectra. Compounds **21a-*D*** and **22a-*D*** were determined to be the exo-adducts as shown in Scheme 4 by the ^{1}H NMR spectrum of the mixture of **21a-*D***, **22a-*D***, and **21a**. Upon oxidative hydrogen abstraction with DDQ and subsequent anion-exchange reaction, a mixture of **21a** and **22a** regenerated **11a**$^+$·BF$_4^-$ in quantitative yield. Upon similar oxidation with DDQ and subsequent anion exchange reaction, a mixture of **21a-*D***, **22a-*D***, and **21a** (in a ratio of 83:2:15) afforded a mixture of deuterated cations, **11a**$^+$**-13*D*·BF$_4^-$**, **11a**$^+$**-11*D*·BF$_4^-$**, and **11a**$^+$·BF$_4^-$ in a ratio of 66:2:32 in quantitative yield (Scheme 5). The ratio was determined by the ^{1}H NMR spectrum of the mixture. While the hydride adduct **21a** regenerated **11a**$^+$·BF$_4^-$, the deuterated adducts **21a-*D*** and **22a-*D*** regenerated a mixture of deuterated cations, **11a**$^+$**-13*D*·BF$_4^-$**, **11a**$^+$**-11*D*·BF$_4^-$**, and **11a**$^+$·BF$_4^-$. Thus, 80% of hydrogen and 20% of deuterium seems to be abstracted from **21a-*D*** and **22a-*D***. The endo-exo selectivity including deuterium isotope effect for the oxidation is obscure. On the other hand, in the reaction of **21b** with DDQ, a trace amount of **11b**$^+$·BF$_4^-$ was obtained in addition to a substantial quantity of unidentified

(34) (a) Paquette, L. A.; Berk, H. C.; Ley, S. V. *J. Org. Chem.* **1975**, *40*, 902 and references therein. (b) Reisdorff, J.; Vogel, E. *Angew. Chem., Int. Ed. Engl.* **1972**, *11*, 218.

SCHEME 5[a]

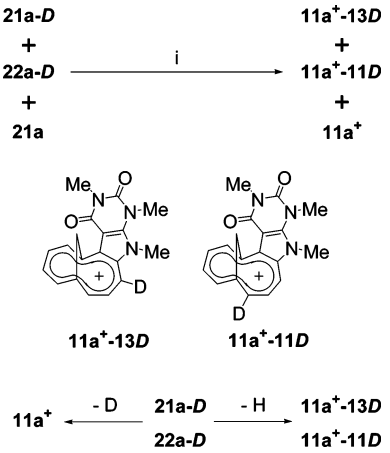

[a] Reagents and conditions: (i) (a) DDQ, CH_2Cl_2, CH_3CN, rt, 30 min; (b) 42% aq HBF_4, Ac_2O, 0 °C, 30 min.

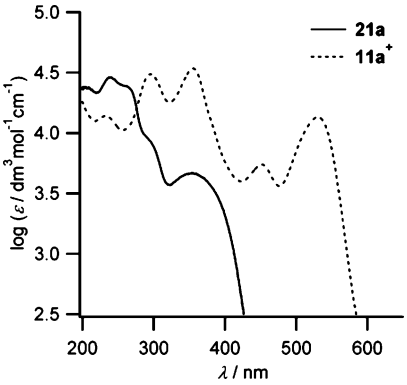

FIGURE 7. UV−vis spectra of **21a** with **11a**$^+$**·BF**$_4^-$.

materials. In addition, photoirradiation of a mixture of **21a** and **22a** in $CD_3CN-CDCl_3$ solution containing 42% aq HBF_4 in an NMR tube under aerobic conditions for 4 h afforded serious decomposition products, and a trace amount of **11a**$^+$**·BF**$_4^-$ was detected. Thus, photoinduced oxidation reaction of **21a** and **22a** to regenerate **11a**$^+$**·BF**$_4^-$ does not take place effectively.

Properties of Hydride Adduct 21a. Recrystallization of a mixture **21a** and **22a** from $CHCl_3/Et_2O$ gave a single crystal of major product **21a**, and thus, hydride adduct **21a** was fully characterized on the basis of the ^{1}H NMR, ^{13}C NMR, IR, UV−vis, and mass spectral data as well as elemental analyses and X-ray crystal analysis. The UV−vis spectra of **21a** in CH_3CN are shown in Figure 7, together with that of **11a**$^+$**·BF**$_4^-$. The longest wavelength absorption maximum (λ_{max}) of **21a** exhibited a blue-shift by 176 nm as compared with that of **11a**$^+$**·BF**$_4^-$, suggesting the contraction of π-conjugation in hydride adduct **21a** (cf. **14**$^+$ and/or **15**$^+$). Unambiguous proton assignment was made by analyzing ^{1}H NMR and H−H COSY spectra. The chemical shifts of bridge protons and selected coupling constants of **21a** are shown in Figure 8. The significant bond alternation of the C6−C7−C8−C9 moiety [$J_{6,7}$ (6.4 Hz), $J_{7,8}$ (10.6 Hz), $J_{8,9}$ (5.6 Hz)] and the large geminal coupling constant of the methylene protons ($J_{E,Z}$ = 12.5 Hz) support the absence of a norcaradiene structure for **21a**. Furthermore, it is interesting that the chemical shifts of the H_Z of **21a** appeared at lower field (δ 3.94) as compared with that of the H_E (δ 0.83). The H_Z of **21a** is located at a deshielding region of the cycloheptatriene moiety and the pyrrole ring moiety. Consequently, the chemical shift of the H_Z appeared at such very low field.

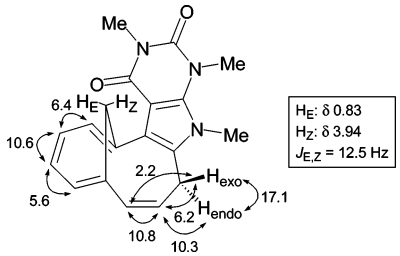

FIGURE 8. Chemical shifts of bridge protons and selected coupling constants of **21a**.

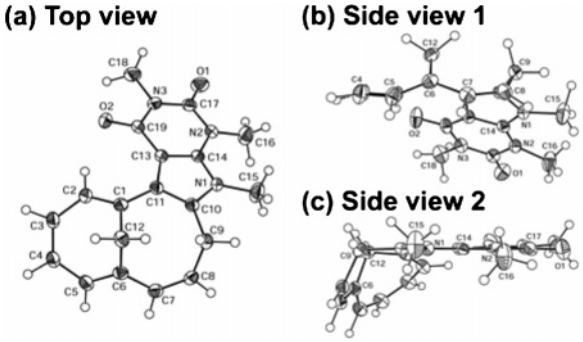

FIGURE 9. ORTEP drawing of **21a** with thermal ellipsoid plot (50% probability). Selected bond lengths (Å) of **21a**: N1−C10 1.407(3), N1−C14 1.359(3), N2−C14 1.377(3), C1−C2 1.369(3), C2−C3 1.428(3), C3−C4 1.370(3), C4−C5 1.426(3), C5−C6 1.360(3), C6−C7 1.452-(3), C7−C8 1.329(3), C8−C9 1.520(3), C9−C10 1.512(3), C10−C11 1.386(3), C11−C13 1.455(3), C13−C14 1.384(3).

To clarify the structural details of **21a**, X-ray crystal analysis was carried out and the ORTEP drawing of **21a** is shown in Figure 9. While the pyrropyrimidine ring moiety of **21a** has a nearly planar structure, large deformation of the bridged 11-membered ring from planarity is observed (Figure 9, side views 1 and 2). It seems that the large deformation makes a distinction between the upside and downside of planarity. Moreover, the C9 of the 11-membered ring of **21a** is closer to the bridged-methylene group, and significant bond alternation is observed in the 11-membered ring. Especially, the bond lengths of C5−C6, C7−C8, and C9−C10 are shorter than those of C6−C7 and C8−C9, suggesting existence of the cycloheptatriene structure for **21a**. The oxidation potentials of **21a** were determined by cyclic voltammentry (CV) in CH_3CN. Two oxidation waves were irreversible under the conditions of the CV measurements; the oxidation waves appeared at +0.56 and +1.53.

Reducing Ability toward Some Carbonyl Compounds. To investigate the reducing ability of **21a,b** and **22a**, reduction of the pyruvate analogue, ethyl benzoylformate, and some carbonyl compounds was carried out in the presence of $Mg(ClO_4)_2$ (Scheme 6). The reaction conditions and the results are summarized in Table 3. The yields were calculated by the ratios of the reduced alcohols and carbonyl compounds obtained by the ^{1}H NMR data of the mixtures. The hydride-adducts **21a** and **22a** reduced ethyl benzoylformate **23** smoothly at rt for 1.5 h to produce ethyl mandelate **26** in quantitative yield (Table 3, entry 1). Generated cation **11a**$^+$ was recovered in 100% yield by converting to a mixture of **21a** and **22a** on treatment with $NaBH_4$. The hydride-adduct **21b** also reduced ethyl benzoylformate **23** at 80 °C for 72 h to give **26** in 67% yield, and generated cation **11b**$^+$ was recovered in 24% yield by converting to **21b** on treatment with $NaBH_4$ (entry 2). The reduction of **23** by using hydride-adducts **21a** and **22a** proceeded more ef-

TABLE 3. Reduction of Some Carbonyl Compounds by Mixtures of 21a and 22a, and 21a-*D* and 22a-*D*, and Pure 21b

entry	hydride adduct	compd carbonyl	*T* (°C)	time (h)	product (yield, %)	recovery of cations[h] (%)
1	**21a**, **22a**[a]	**23**	rt[c]	1.5	**26** (100)	100
2	**21b**	**23**	80[d]	72	**26** (67), **23** (33)[g]	24
3	**21a**, **22a**[a]	**24**	rt[c]	2	**27** (88), **24** (12)[g]	100
4	**21a**, **22a**[a]	**24**	60[e]	2	**27** (96), **24** (4)[g]	82
5	**21a**, **22a**[a]	**25**	60[e]	15	**28** (99), **25** (1)[g]	100
6	**21a-*D***, **22a-*D***[b]	**23**	rt[f]	3	**26-*D*** (96), **26** (4)[g]	100

[a] A mixture of **21a** and **22a** in a ratio of 81:19. [b] A mixture of **21a-*D***, **22a-*D***, and **21a** in a ratio of 83:2:15. [c] $CH_2Cl_2-CH_3CN$ (2/1) was used. [d] $(CH_2Cl)_2-CH_3CN$ (1/1) was used. [e] $CHCl_3-CH_3CN$ (2/1) was used. [f] $CH_2Cl_2-CH_3CN$ (1/2) was used. [g] The yield was determined from the ^1H NMR spectrum of the mixture. [h] Isolated by converting to mixtures of **21a** and **22a**, **21a-*D***, **22a-*D***, and **21a**, and pure **21b** by treatment with $NaBH_4$ or $NaBD_4$.

SCHEME 6[a]

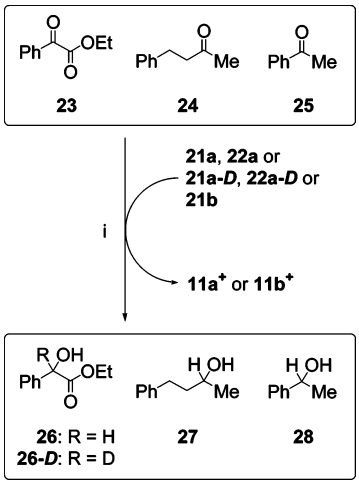

[a] Reagents and conditions: (i) $Mg(ClO_4)_2$, in the dark, conditions listed in Table 3.

ficiently as compared with that of **21b**, and thus, **21a** and **22a** were used for the further reactions. We found that **21a** and **22a** have reducing ability toward 4-phenyl-2-butanone **24** and acetophenone **25**. The reduction of dialkylated ketone **24** by using **21a** and **22a** at rt for 2 h afforded 4-phenyl-2-butanol **27** in good yield (88%, entry 3); however, the yield was not improved by the prolonged reaction time. By raising temperature (at 60 °C), the reduction of **24** proceeded smoothly to give **27** in 96% yield (entry 4). In addition, the hydride-adducts **21a** and **22a** reduced aromatic ketone **25** at 60 °C for 15 h to give 1-phenylethanol **28** in good yield (99%, entry 5). These facts show that **21a** and **22a** could reduce activated ketone, aliphatic ketone as well as aromatic ketone. To clarify the exo or endo selectivity of the hydride, which intervenes in the carbonyl reduction, the reduction of **23** with deuterated adducts **21a-*D*** and **22a-*D*** was carried out. The deuterated adducts **21a-*D*** and **22a-*D*** (containing **21a**) reduced **23** at rt to give the corresponding deuterated alcohol **26-*D*** and **26** in 96% and 4% yields, respectively (entry 6). Thus, the deuteride located at the exo-position of **21a-*D*** and **22a-*D*** was mainly used to reduce **23**, suggesting that the methano-bridge controls the reaction. This feature is very interesting in considering the DDQ-oxidation reaction of a mixture of **21a-*D***, **22a-*D***, and **21a** (vide supra); the deuteride located at the exo-position of **21a-*D*** and **22a-*D*** mainly used for reduction of **23** and deuterated alcohol **26-*D*** was obtained as the major product. Thus, the reduction of carbonyl compounds using **21a** and **22a** would proceed via hydride transfer process. This is the first example of the reduction of carbonyl compounds by a methano[11]annulenylium system, and provides promising possibility for the exploration of chiral reduction systems.

Summary

A synthesis of novel cations **11a,b**$^+\cdot BF_4^-$, which are catacondensed with pyrrolo[2,3-*d*]pyrimidine-1,3(2,4*H*)-dione toward **7**$^+$, was accomplished. Structural characteristics of **11a,b**$^+$ were clarified on inspection of the UV−vis and NMR spectral data as well as X-ray crystal analyses. The stability of cations **11a,b**$^+$ is expressed by the pK_{R+} values which were determined spectrophotometrically as 9.8 and 9.7, respectively. The electrochemical reduction of **11a,b**$^+\cdot BF_4^-$ exhibited reduction potential at −0.58 and −0.52 (V vs $Ag/AgNO_3$). The photoinduced oxidation reaction of **11a,b**$^+\cdot BF_4^-$ toward some amines under aerobic conditions was carried out to give the corresponding imines with the recycling number of 1.1 to 32.2. While the hydride reduction of **11a**$^+\cdot BF_4^-$ afforded a mixture of the C13-adduct **21a** and the C11-adduct **22a**, similar reaction of **11b**$^+\cdot BF_4^-$ afforded only C13-adduct **21b**. In both reactions, the methano-bridge controls the hydride attack which occurs preferentially with exo-selectivity. The reduction of some carbonyl compounds including a pyruvate analogue was accomplished by using **21a** and **22a**; and thus, a novel NADH model system is postulated. Further studies including the mechanistic aspect and enantioselective reduction of carbonyl compounds will be reported in due course.

Experimental Section

Preparation of 11a$^+\cdot BF_4^-$ **by Methylation of 10a.** A solution of **10a** (91.5 mg, 0.30 mmol) and MeI (6 mL) in $(CH_2Cl)_2$ (15 mL) was heated in a sealed tube at 100 °C for 48 h. Then, more MeI (6 mL) was added to the solution, and it was heated at 100 °C for further 48 h. Finally, more MeI (3 mL) was added to the solution and it was heated at 100 °C for 3 h. After evaporation of the solvent, the residue was dissolved in a mixture of Ac_2O (10 mL), CH_3CN (4 mL), and 42% aq. HBF_4 (2 mL) at 0 °C, and the mixture was stirred for 30 min. To the mixture was added Et_2O (200 mL) and the precipitates were collected by filtration and washed with Et_2O to give **11a**$^+\cdot BF_4^-$ (122 mg, 100%). Dark red crystals (120 mg, 98%) were obtained on recrystallization by slow evaporation of the solvents from CH_3CN/Et_2O.

Preparation of 11b$^+\cdot BF_4^-$ **by Methylation of 10b.** A solution of **10b** (24.2 mg, 0.066 mmol) and MeI (1.3 mL) in $(CH_2Cl)_2$ (3.3 mL) was heated in a sealed tube at 100 °C for 29 h. Then, more MeI (1.3 mL) was added to the solution and it was heated at 100 °C for further 19 h. After evaporation of the solvent, the residue was dissolved in a mixture of Ac_2O (3 mL) and 42% aq. HBF_4 (0.6 mL) at 0 °C, and the mixture was stirred for 30 min. To the mixture was added Et_2O (100 mL) and the precipitates were collected by filtration and washed with Et_2O to give **11b**$^+\cdot BF_4^-$ (30.9 mg, 100%).

Preparation of 11b$^+\cdot BF_4^-$ **Starting from 7**$^+$**.** A mixture of **12** (46.2 mg, 0.20 mmol) and K_2CO_3 (278 mg, 2.0 mmol) in CH_3CN (3 mL) was stirred at rt for 1 h. To the mixture was added a solution of **7**$^+\cdot BF_4^-$ (48.4 mg, 0.20 mmol) in CH_3CN (2 mL) dropwise,

and the mixture was stirred at rt for 48 h to give **13**. After evaporation of the solvent, the residue was neutralized with saturated aqueous NH_4Cl and extracted with CH_2Cl_2, and the extract was dried over Na_2SO_4. After evaporation of the solvent, to the residue dissolved in CH_3CN (5 mL) was added DDQ (90.8 mg, 0.40 mmol), and the mixture was stirred at rt for 1 h. After evaporation of the solvent, the residue was dissolved in a mixture of Ac_2O (5 mL) and 42% aq. HBF_4 (1 mL) at 0 °C and stirred for 30 min. To the mixture was added Et_2O (200 mL) and the precipitates were collected by filtration and washed with Et_2O to give **11b**$^+$**·BF**$_4^-$ (75.9 mg, 81%).

Determination of pK_{R+} Value of 11a,b$^+$. Buffer solutions of slightly different acidities were prepared by mixing aqueous solutions of $Na_2B_4O_7$ (0.025 M) and HCl (0.1 M) (for pH 8.2−9.0), $Na_2B_4O_7$ (0.025 M) and NaOH (0.1 M) (for 9.2−10.8), and Na_2HPO_4 (0.05 M) and NaOH (0.1 M) (for pH 11.0−12.0) in various portions. For the preparation of sample solutions, 1 mL portions of the stock solution, prepared by dissolving 16 mg of compound **11a,b**$^+$**·BF**$_4^-$ in CH_3CN (50 mL), were diluted to 10 mL with the buffer solution (8 mL) and CH_3CN (1 mL). The UV−vis spectrum was recorded for cation **11a,b**$^+$**·BF**$_4^-$ in 20 different buffer solutions. Immediately after recording the spectrum, the pH of each solution was determined on a pH meter calibrated with standard buffers. The observed absorbance at the specific absorption wavelength (531 nm for **11a**$^+$**·BF**$_4^-$; 527 nm for **11b**$^+$**·BF**$_4^-$) of cation **11a,b**$^+$**·BF**$_4^-$ was plotted against pH to give a classical titration curve, whose midpoint was taken as the pK_{R+} value.

General Procedure for Autorecycling Oxidation of Amines in the Presence of 11a,b$^+$·BF$_4^-$. A CH_3CN (16 mL) solution of compound **11a,b**$^+$**·BF**$_4^-$ (**11a**$^+$**·BF**$_4^-$: 2.034 mg, 5 μmol, **11b**$^+$**·BF**$_4^-$: 2.344 mg, 5 μmol) and amines (2.5 mmol, 500 eq.) in a Pyrex tube was irradiated by RPR-100, 350 nm lamps under aerobic conditions for 16 h. The reaction mixture was concentrated in vacuo and diluted with Et_2O and filtered. The ^{1}H NMR spectra of the filtrates revealed the formation of the corresponding imines. The filtrate was treated with saturated solution of 2,4-dinitrophenylhydrazine in 6% HCl to give 2,4-dinitrophenylhydrazone of the corresponding carbonyl compounds. The results are summarized in Table 2.

Reaction of 11a,b$^+$·BF$_4^-$ with NaBH$_4$. A solution of **11a,b**$^+$**·BF**$_4^-$ (**11a**$^+$**·BF**$_4^-$: 10.2 mg, 0.025 mmol; **11b**$^+$**·BF**$_4^-$: 31.3 mg, 0.067 mmol) and $NaBH_4$ (2.6 equiv) in CH_3CN (5 mL) was stirred at rt for 30 min. To the mixture was added saturated aqueous NH_4Cl solution, and the mixture was extracted with CH_2Cl_2. The CH_2Cl_2 extract was dried over Na_2SO_4 and concentrated in vacuo to give **21a** and **22a** in a ratio of 81:19 (8.0 mg, 100%) and **21b** (25.7 mg, 100%). The ratio of **21a** and **22a** was assessed by measurement of the integrated signals of the ^{1}H NMR spectrum of the H12 at δ = 4.38 ppm (ddd) for **21a** and the H12 at δ = 4.48 ppm (ddd) for **22a**. See the Supporting Information (S23−S25).

Reaction of 11a$^+$·BF$_4^-$ with NaBD$_4$. A solution of **11a**$^+$**·BF**$_4^-$ (10.2 mg, 0.025 mmol) and $NaBD_4$ (2.7 mg, 0.065 mmol) in CH_3CN (5 mL) was stirred at rt for 30 min. To the mixture was added saturated aqueous NH_4Cl solution, and the mixture was extracted with CH_2Cl_2. The CH_2Cl_2 extract was dried over Na_2SO_4 and concentrated in vacuo to give a mixture of **21a-*D***, **22a-*D***, and **21a** in a ratio of 83:2:15 (8.1 mg, 100%). The ratio was assessed by measurement of the integrated signals of the ^{1}H NMR spectrum of the H6 at δ = 8.12 ppm (d) for **21a-*D*** and the H6 at δ = 8.18 ppm (d) for **22a-*D*** and the H12 at δ = 4.41 ppm (ddd) for **21a**. See the Supporting Information (S26−S28).

Oxidation of 21a and 22a. To a stirred solution of **21a** and **22a** (in a ratio of 81:19, 8.0 mg, 0.025 mmol) in a mixture of CH_2Cl_2 (3 mL) and CH_3CN (3 mL) was added DDQ (24.0 mg, 0.11 mmol), and the mixture was stirred at rt for 30 min. After evaporation of CH_2Cl_2, the residue was dissolved in a mixture of CH_3CN (1 mL), Ac_2O (2 mL), and 42% aq HBF_4 (0.4 mL) at 0 °C, and the mixture was stirred for another 30 min. To the mixture was added Et_2O (100 mL) and the precipitate was collected by filtration to give **11a**$^+$**·BF**$_4^-$ (10 mg, 98%).

Oxidation of 21a-*D* and 22a-*D*. To a stirred solution of a mixture of **21a-*D***, **22a-*D***, and **21a** (in a ratio of 83:2:15, 8.1 mg, 0.025 mmol) in CH_2Cl_2 (3 mL) and CH_3CN (3 mL) was added DDQ (12 mg, 0.053 mmol), and the mixture was stirred at rt for 30 min. After evaporation of CH_2Cl_2, the residue was dissolved in a mixture of CH_3CN (1 mL), Ac_2O (2 mL), and 42% aq HBF_4 (0.4 mL) at 0 °C, and the mixture was stirred for another 30 min. To the mixture was added Et_2O (100 mL), and the precipitate was collected by filtration to give a mixture of deuterated cations, **11a**$^+$**-13*D*·BF**$_4^-$, **11a**$^+$**-11*D*·BF**$_4^-$, and **11a**$^+$**·BF**$_4^-$ in a ratio of 66:2:32 (10.2 mg, 100%). The ratio was assessed by measurement of the integrated signals of the ^{1}H NMR spectrum of the H13 at δ = 8.99 ppm (d) for a mixture of **11a**$^+$**-11*D*·BF**$_4^-$ and **11a**$^+$**·BF**$_4^-$ and the H11 at δ = 8.94 ppm (d) for a mixture of **11a**$^+$**-13*D*·BF**$_4^-$ and **11a**$^+$**·BF**$_4^-$ and the H6 at δ = 10.23 ppm (d) for a mixture of **11a**$^+$**-13*D*·BF**$_4^-$, **11a**$^+$**-11*D*·BF**$_4^-$, and **11a**$^+$**·BF**$_4^-$. See the Supporting Information (S29−S30).

Cyclic Voltammetry of Cations 11a,b$^+$ and Hydride Adduct 21a. The reduction potential of **11a,b**$^+$ and **22** was determined by means of CV-27 voltammetry controller (BAS Co). A three-electrode cell was used, consisting of Pt working and counter electrodes and a reference $Ag/AgNO_3$ electrode. Nitrogen was bubbled through a CH_3CN solution (4 mL) of cation **11a,b**$^+$**·BF**$_4^-$ (0.5 mM) and **21a** (0.5 mM) and Bu_4NClO_4 (0.1 M) to deaerate it. The measurements were made at a scan rate of 0.1 V s^{-1} and the voltammograms were recorded on a WX-1000-UM-019 (Graphtec Co) X−Y recorder. Immediately after the measurements, ferrocene (0.1 mmol) ($E_{1/2}$ = +0.083) was added as the internal standard, and the observed peak potential was corrected with reference to this standard. The cation **11a,b**$^+$**·BF**$_4^-$ exhibited reduction waves, respectively, and they are summarized in Table 2.

Reduction of Some Carbonyl Compounds by Using 21a and 22a, 21a-*D* and 22a-*D*, and 21b. To a solution of mixtures **21a** and **22a**, **21a-*D***, **22a-*D***, and **21a**, and pure **21b** (0.1 mmol) and $Mg(ClO_4)_2$ (22 mg, 0.1 mmol) in CH_3CN (5 mL) and CH_2Cl_2 (10 mL) or $CHCl_3$ (10 mL) or $(CH_2Cl)_2$ (5 mL) in a sealed tube was added **23**, **24**, and **25** (0.1 mmol), and the mixture was stirred in the dark under the conditions indicated in Table 3. To the resulting mixture was added AcOH (6 mg, 0.1 mmol) and the mixture concentrated in vacuo. The residue was dissolved in Et_2O, and the precipitated crystals were collected by filtration. The filtrate was concentrated in vacuo to give a reduced alcohol derivative or a mixture of carbonyl compound and alcohol derivative as summarized in Table 3. On the other hand, the collected crystals containing **11a,b**$^+$**·ClO**$_4^-$ were dissolved in CH_3CN and reacted with $NaBH_4$ (10 mg, 0.26 mmol) or $NaBD_4$ (11 mg, 0.26 mmol), and stirred at rt for 30 min. To the mixture was added saturated aqueous NH_4Cl solution, and the mixture was extracted with CH_2Cl_2. The extract was dried over Na_2SO_4 and concentrated in vacuo to recover mixtures **21a** and **22a**, **21a-*D***, **22a-*D***, and **21a**, and pure **21b** as summarized in Table 3.

Acknowledgment. Financial support from a Waseda University Grant for Special Research Project and 21COE "Practical Nano-chemistry" from MEXT, Japan, is gratefully acknowledged. We thank the Materials Characterization Central Laboratory, Waseda University, for technical assistance with the spectral data, elemental analyses, and X-ray analyses.

Supporting Information Available: Physical, analytical, and spectroscopic data of **11a,b**$^+$**·BF**$_4^-$, **21a,b**, **21a-*D***, and **11a**$^+$**-13*D*·BF**$_4^-$. ^{1}H and ^{13}C NMR spectra of **11a,b**$^+$**·BF**$_4^-$ and **21a,b**. This material is available free of charge via the Internet at http://pubs.acs.org.

JO052495M